Available online at www.sciencedirect.com
SCIENCE DIRECT®
International Journal of Heat and Mass Transfer 47 (2004) 3279–3290
International Journal of HEAT and MASS TRANSFER
www.elsevier.com/locate/ijhmt

Radiation effects on transient hot-wire measurements in absorbing and emitting porous media

Ulrich Gross [a,*], Le-Thanh-Son Tran [b]

[a] Institut für Wärmetechnik und Thermodynamik, Technische Universität Bergakademie Freiberg, Gustav-Zeuner-Str. 7, 09599 Freiberg, Germany

[b] Robert Bosch GmbH, DS-NF/EAN2, Wernerstrasse 51, 70469 Stuttgart, Germany

Received 27 November 2003; received in revised form 2 February 2004
Available online 9 April 2004

Abstract

The integro-differential equation governing the combined conduction and radiation heat transfer in a gray medium bounded by two infinite coaxial cylindrical surfaces is solved numerically to analyse the effect of radiation in transient hot-wire measurements in porous thermal insulations. The influences of the extinction coefficient, the emissivity of the wire and the heating power are studied. It is found that the hot-wire method works accurately only in cases where the extinction coefficient exceeds a minimum value which increases with the temperature. The calculated results confirm the linear relationship between measured thermal conductivities and the heating power. The problem of reference temperature for the measured thermal conductivity is also discussed in this work.

Keywords: Transient hot-wire method; Radiation; Porous media; Thermophysical properties; Numerical analysis; Discrete ordinates method

1. Introduction

The transient hot-wire method described by Healy et al. [1] has been developed rapidly since many years. Generally, this method has the advantages of convenience, accuracy and short duration of the measurement. It has been widely used for determination of the thermal conductivity of fluids and solids. The basic method, however, is restricted to cases of exclusively conductive heat transfer without any convection and no emission, absorption and scattering of radiation. Such substances are either completely opaque or ideally transparent.

In cases of reduced transparency of the medium, there is an additional transport due to radiation which is emitted at any location inside the medium and absorbed again after repeated scattering within a certain free mean path, i.e. the penetration length. This is the inverse of the extinction coefficient as the sum of the coefficients for absorption and scattering. Heat transfer is now a coupled process of conduction and radiation which can be described by means of the effective thermal conductivity including both effects. This however is only allowed if radiation is a local, diffusion-like process where the extinction coefficient is large enough, i.e. in optically dense materials. In such cases the hot-wire method can be applied and the effective thermal conductivity is yielded as the sum of two contributions namely one term for thermal conduction (i.e. the thermal conductivity) and a second one for radiation (the so-called radiative conductivity).

If the extinction coefficient is small, however, with weak emission and absorption as found in some fluids, heat transfer does only approximately correspond to the governing equation of the transient hot-wire method. By this an apparent thermal conductivity will be measured and the application of correction terms has been suggested for getting the true and radiation-free thermal conductivity. Respective analytical investigations are

* Corresponding author. Tel.: +49-3731-392684; fax: +49-3731-393655.
E-mail address: gross@iwtt.tu-freiberg.de (U. Gross).

0017-9310/$ - see front matter © 2004 Elsevier Ltd. All rights reserved.
doi:10.1016/j.ijheatmasstransfer.2004.02.014

Nomenclature

c_p	heat capacity [J/kg K]
C	constant, $C = e^{\gamma} = 1.781$
E	extinction coefficient [1/m]
I	radiation intensity [W/m^2 sr]
$J_{0,1}$, $Y_{0,1}$	Bessel functions (1st and 2nd kind respectively)
k_a	absorption coefficient [1/m]
k_s	scattering coefficient [1/m]
l_m	mean penetration length [m]
M	number of discrete directions
N	level number of the discrete ordinates method
n	index of refraction
$\dot{q}$	heat flux [W/m^2]
$\dot{Q}_l$	heating power per unit length [W/m]
r	radius [m]
s	coordinate along path of radiation [m]
t	time [s]
T	temperature [K]
w_i	weights

Greek symbols

α_i	coefficients
β_i	roots
ε	emissivity
η, μ, ξ	direction cosines
κ	thermal diffusivity [m^2/s]
λ	thermal conductivity [W/m K]
θ	polar angle
ϑ	temperature [°C]
ρ	mass density [kg/m^3]
σ	Stefan–Boltzmann constant
ψ	azimuthal angle
Ω	solid angle [sr]

Subscripts

b	blackbody
c	conductive
eff	effective
m	mean value
r	radiative
s	outer boundary of the sample
w	hot wire
0	initial value

reported, e.g., by Saito and Venart [2], Saito [3], Menashe and Wakeham [4] and de Castro et al. [5] for radiation effects upon transient hot-wire measurements of liquids.

The determination of the required critical minimum of the extinction coefficient is only possible with the numerical simulation of the measuring procedure. For this purpose, Ebert and Fricke [6] solved the governing energy equation of the combined conduction and radiation problem by the method of successive approximation. For the boundary condition at the wire, the authors neglected radiation emitted from the wire surface. The radiation transport problem was solved by application of the Milne–Eddington approximation which only works accurately for optically thick media. As the result, the authors found $E = 15,000$/m as the lower limit of the extinction coefficient, which must be exceeded for application of the diffusion model where the effective thermal conductivity can be determined from the hot-wire data.

In order to analyse this heat transfer process in more detail and more accuracy, the radiation emitted from the wire will be taken into account for the boundary condition at the wire and the radiation transport equation will be solved by means of the discrete ordinates method which is suitable for both optically thick and optically thin media, i.e. for high and for low extinction coefficients. The coupled differential equations for energy and radiation transfer will then be solved numerically with the finite difference method.

Onset of convection and related effects which are of outstanding importance in case of fluids will not be considered here as it plays a negligible role in porous media.

2. The principle of transient hot-wire measurements

2.1. Fundamentals

The transient hot-wire method uses a thin electrically heated wire immersed in the sample as a line source to generate a transient temperature field in the measured medium when a constant heating power is applied to the wire. The fundamental differential equation governing the line-source problem

$$\rho c_p \frac{\partial T}{\partial t} = -\nabla \cdot \dot{\bar{q}}_c = \nabla \cdot (\lambda_c \nabla T), \tag{1}$$

is subjected to boundary conditions

$$\text{at } t \leqslant 0 \text{ and any } r \quad \Delta T(r,t) = 0, \tag{2}$$

$$\text{at } r = r_w \text{ and any } t \geqslant 0 \quad \frac{\dot{Q}_l}{2\pi r_w} = -\lambda_c \left(\frac{\partial T}{\partial r}\right)_{r=r_w}, \tag{3}$$

$$\text{at } r \to \infty \text{ and any } t \geqslant 0 \quad \lim_{r\to\infty} \Delta T(r,t) = 0 \tag{4}$$

assuming

$$\rho = \text{const}, \quad c_p = \text{const}, \quad \lambda_c = \text{const}, \tag{5}$$

where T is the temperature, t the time, ρ the density, c_p the specific heat and λ_c the thermal conductivity of the medium. For a sufficiently small radius of the wire r_w and long times t, i.e. for $r_w^2/(4\kappa t) \ll 1$, the solution of the Eqs. (1)–(4) can be obtained as follows [1]:

$$\Delta T = \frac{\dot{Q}_l}{4\pi\lambda_c} \ln\left(\frac{4\kappa t}{r_w^2 C}\right), \tag{6}$$

where ΔT is the temperature rise of the wire, $\dot{Q}_l$ the heating power per unit length, κ the thermal diffusivity of the medium, and $C = e^{\gamma} = 1.781$ with Euler's constant γ. Measurements in liquids and gases are restricted to very short times (in the order of some seconds) due to onset of convection, and the criterion $r_w^2/(4\kappa t) \ll 1$ can only be met by using an extremely thin wire (typically $r_w = 5$ μm and below). Application of the hot-wire method to solids, however, requires a mechanically stable wire with a radius ranging up to $r_w = 250$ μm, and consequently much longer measuring times (typically up to 600 s) are needed. In case of porous solids, the onset of convection depends on pore structure (open or closed pores and their size) and it is restricted to very high temperature differences which are never attained in practice.

Analytically, two temperatures T_1 and T_2 measured at times t_1 and t_2, should be sufficient to get the thermal conductivity, λ_c:

$$\lambda_c = \frac{\dot{Q}_l}{4\pi} \cdot \frac{\ln t_2 - \ln t_1}{T_2 - T_1}. \tag{7}$$

Eq. (7) is used as the evaluation procedure of the transient hot-wire method and it works accurately in media with exclusively conduction heat transfer.

2.2. Application to participating media

The combined conduction and radiation heat transfer in transient hot-wire measurements is described by the balance of energy:

$$\rho c_p \frac{\partial T}{\partial t} = \nabla \cdot (\lambda_c \nabla T) - \nabla \cdot \dot{q}_r, \tag{8}$$

including now the radiation term, $\nabla \cdot \dot{q}_r$:

$$\nabla \cdot \dot{q}_r = k_a\left(4\sigma T^4 - \int_{4\pi} I \, d\Omega\right), \tag{9}$$

as the difference of emitted and absorbed radiation, where $\dot{q}_r$ is the radiative flux, k_a the absorption coefficient of the medium, σ the Stefan–Boltzmann constant, I the intensity of radiation and Ω the solid angle. Eq. (8) is subjected to boundary conditions

$$\text{at } t \leqslant 0 \text{ and any } r \quad \Delta T(r,t) = 0, \tag{10}$$

$$\text{at } r = r_w \text{ and any } t \geqslant 0 \quad \frac{\dot{Q}_l}{2\pi r_w} = -\lambda_c\left(\frac{\partial T}{\partial r}\right)_{r=r_w} + \dot{q}_r, \tag{11}$$

$$\text{at } r = r_s \text{ and any } t \geqslant 0 \quad \Delta T(r_s,t) = 0. \tag{12}$$

The problem of combined conduction and radiation heat transfer deviates from the fundamentals of the line-source technique because radiation terms are present in Eq. (8), $\nabla \cdot \dot{q}_r$, and in the boundary condition (11), $\dot{q}_r$. In order to use the solution (7) of the line-source technique for evaluation of the measured results of conducting, emitting and absorbing media, it is necessary that the radiation term can be converted in such a way that Eqs. (8) and (11) correspond to the respective expressions of the fundamental line-source technique. This is possible with the diffusion model by which the radiative heat flux, $\dot{q}_r$, can be rewritten as:

$$\dot{q}_r = -\lambda_r \frac{\partial T}{\partial r}, \tag{13}$$

and divergence of the radiative heat flux, $\nabla \cdot \dot{q}_r$, as:

$$\nabla \cdot \dot{q}_r = -\nabla \cdot (\lambda_r \nabla T). \tag{14}$$

In Eqs. (13) and (14), λ_r is the radiative conductivity defined by [7]:

$$\lambda_r = \frac{16 n^2 \sigma}{3E} \cdot T_r^3, \tag{15}$$

where E is the extinction coefficient. For an absorbing and emitting medium without scattering the extinction coefficient, E, is equal to the absorption coefficient, k_a. Substituting Eq. (14) into (8) and Eq. (13) into (11) we get

$$\rho c_p \frac{\partial T}{\partial t} = \nabla \cdot (\lambda_{\text{eff}} \nabla T) \tag{16}$$

and

$$\frac{\dot{Q}_l}{2\pi r_w} = -\lambda_{\text{eff}}\left(\frac{\partial T}{\partial r}\right)_{r=r_w}, \tag{17}$$

respectively with $\lambda_{\text{eff}} = \lambda_c + \lambda_r$ as the effective thermal conductivity of the conducting, emitting and absorbing medium. It is quite obvious that the structure of Eqs. (16) and (17) are identical with those of Eqs. (1) and (3) respectively. With this similarity, measurements of the effective thermal conductivity of conducting, emitting and absorbing media by the transient hot-wire method seems to be possible.

Before the method is actually used, we have to check its applicability with respect to the validity of the diffusion model. Although Eq. (16) holds for optically thick media [7], Eq. (17) as the wire-side boundary condition will cause errors as the diffusion model is not valid close to some boundary of the medium [7,8]. It can be

considered as an approximation for strongly absorbing media. The at least necessary absorption coefficient can only be determined by numerical simulation of the transient hot-wire experiment.

3. Numerical analysis of the conduction–radiation problem

3.1. Assumptions of the model

With respect to the solubility of the combined processes of conduction and radiation heat transfer, the following assumptions are made:

(a) The medium is isotropic, homogeneous and infinitely extended in axial direction. Thermal conductivity, λ_c, density, ρ, and specific heat, c_p, of the medium are constant, i.e. they do not depend on temperature.
(b) The medium is bounded by two infinite coaxial cylinders. The inner cylinder describes the hot-wire surface with radius r_w and the radius r_s marks the isothermal outside boundary of the sample at temperature T_0.
(c) The hot-wire surface is diffusely reflecting and has a constant emissivity ε_w. The outer sample boundary is black ($\varepsilon_s = 1$). The sample is every time in local thermal equilibrium.
(d) The radiative heat transfer is free of inertia effects and it can be described by the steady-state solution.
(e) The medium is gray and has constant IR-optical properties, i.e. the absorption coefficient, k_a, the scattering coefficient, k_s, and the index of refraction, n.
(f) At time $t = 0$ the wire and the medium are isothermal at temperature T_0.

3.2. Radiation transport equation

The conduction–radiation problem is governed by a system of two equations, namely the energy balance, Eq. (8), including the radiation term, Eq. (9), and the balance of monochromatic radiation passing through a volume element, which contains an absorbing, emitting, scattering and gray medium, written as [7]

$$\frac{\mathrm{d}I}{\mathrm{d}s} = \vec{s}\cdot\nabla I = -(k_a + k_s)I + k_a I_b + \frac{k_s}{4\pi}\int_{4\pi} I(\vec{s}')\Phi(\vec{s}\cdot\vec{s}')\,\mathrm{d}\Omega'. \quad (18)$$

The left side of Eq. (18) represents the gradient of intensity in the direction of propagation, the right-hand side includes, respectively, the attenuation of intensity due to absorption and out-scattering, and the contribution to the directional intensity due to emission by the medium, and in-scattering from various directions expressed by the phase function $\Phi(\vec{s}\cdot\vec{s}')$.

Eqs. (8) and (18) are coupled due to the last term in Eq. (9) which accounts for absorption of irradiated energy to be calculated from Eq. (18), and on the other hand due to the emission term in Eq. (9) which depends on the local temperature.

Eq. (18) forms the basis for all radiation calculations and it can be written for axisymmetric cylindrical media as

$$\sin\theta\cos\psi\frac{\partial I}{\partial r} - \frac{\sin\theta\sin\psi}{r}\frac{\partial I}{\partial\psi} = -(k_a + k_s)I + k_a I_b + \frac{k_s}{4\pi}\int_{4\pi} I(\vec{s}')\Phi(\vec{s}\cdot\vec{s}')\,\mathrm{d}\Omega', \quad (19)$$

where the polar angle θ is measured from the z-axis (i.e. the symmetry axis), and the azimuthal angle ψ is measured from the local radial direction. Introducing the direction cosines, $\xi = \vec{s}\cdot\vec{e}_z = \cos\theta$, $\mu = \vec{s}\cdot\vec{e}_r = \sin\theta\cos\psi$, and $\eta = \vec{s}\cdot\vec{e}_{\psi_c} = \sin\theta\sin\psi$, we can rewrite Eq. (19) as

$$\frac{\mu}{r}\frac{\partial(rI)}{\partial r} - \frac{1}{r}\frac{\partial(\eta I)}{\partial\psi} = -(k_a + k_s)I + k_a I_b + \frac{k_s}{4\pi}\int_{4\pi} I(\vec{s}')\Phi(\vec{s}\cdot\vec{s}')\,\mathrm{d}\Omega' \quad (20)$$

This equation has now to be solved by a proper method which must be suitable for extensive parameter studies. Due to the mathematical complexity of cylindrical geometry, only a few studies have been made. Saito and Venart [2] used a modified integral method for solving the differential equation of energy. However, the authors calculated the radiative flux as an approximation from the temperature distribution for the conduction case that cannot consider sufficiently the interaction between conduction and radiation. Menashe and Wakeham [4] solved numerically the full integro-partial differential equation governing the simultaneous conduction–radiation process in a transient hot-wire cell for the characteristics of liquids. Ebert and Fricke [6] applied the Milne–Eddington approximation for the radiation transport, the application of which however, is limited to very high absorption coefficients. Yu et al. [9] solved the full integro-differential energy equation numerically with the control volume method.

In order to carry out extensive parameter studies for analysing the radiation effect in transient hot-wire measurements, it is necessary to apply a method for the solution of the radiation transport equation which is fast enough and sufficiently accurate. For this purpose, the discrete ordinates method has been selected.

3.3. Application of the discrete ordinates method

In the discrete ordinates method, Eq. (20) is solved with a finite number of directions spanning the total solid angle of 4π steradians. This number of directions

depends on the order of the discrete ordinates approximation, expressed by the relationship $M = N(N+2)$, where N represents the order of approximation (i.e. the number N of values for the direction cosines to be considered within the range ± 1.0). Therefore, this method is also known as S_N-approximation. The angular integral is evaluated by application of the numerical quadrature. Each discrete direction $\vec{s}_i$ is depicted as a point on the surface of a unit sphere with which a surface area w_i is associated. w_i can be treated as the angular quadrature weight, with the requirement

$$\sum_i w_i = 4\pi. \tag{21}$$

Eq. (20) may then be written in discrete ordinates form as

$$\frac{\mu_i}{r}\frac{\partial(rI_i)}{\partial r} - \frac{1}{r}\frac{\partial(\eta_i I_i)}{\partial \psi} = -(k_a + k_s)I_i + k_a I_b + \frac{k_s}{4\pi}\int_{4\pi} I_{i'}\Phi(\vec{s}\cdot\vec{s}')\,\mathrm{d}\Omega', \tag{22}$$

where $i = 1, 2, \ldots, M$. The angular derivation term in Eq. (22) can be simplified by using the direct-differencing technique proposed by Carlson and Lathrop [10]. By this the second term on the left-hand side of Eq. (22) can be rewritten as

$$\frac{1}{r}\frac{\partial(\eta_i I_i)}{\partial \psi} = \frac{\alpha_{i+1/2}I_{i+1/2} - \alpha_{i-1/2}I_{i-1/2}}{r w_i}. \tag{23}$$

The directions $i \pm 1/2$ define the edges of the angular range of w_i, the two terms representing, respectively, the flow out of and into the angular range. A direct relationship between α_i and w_i can be drawn on the basis of isotropic radiation

$$\alpha_{i+1/2} - \alpha_{i-1/2} = w_i\frac{\partial \eta_i}{\partial \psi} = w_i\mu_i, \tag{24}$$

where $\alpha_{1/2} = 0$ and $\alpha_{M+1/2} = 0$.

Assuming the scatter to be linearly anisotropic, the phase function may be represented by [11]

$$\Phi(\vec{s},\vec{s}') = 1 + a_1\mu_i\mu_{i'}, \tag{25}$$

where a_1 is an anisotropic factor.

Multiplying both sides of Eq. (22) by $2\pi r\,\mathrm{d}r$, and integrating along the radial extention from r_j to r_{j+1}, we obtain

$$\mu_i(A_{j+1}I_{i,j+1} - A_jI_{i,j}) - (A_{j+1} - A_j) \times \frac{\alpha_{i+1/2}I^0_{i+1/2} - \alpha_{i-1/2}I^0_{i-1/2}}{w_i} = -B(k_a + k_s)I^0_i + Bk_aI^0_b + Bk_sI^0_s, \tag{26}$$

where $A_j = 2\pi r_j$, $B = \pi(r^2_{j+1} - r^2_j)$, $I^0_s = \frac{1}{4\pi}\sum_{i'} w_{i'}I^0_{i'}(1 + a_1\mu_i\mu_{i'})$ and the quantities with the superscript 0 denote values at the center of the range from r_j to r_{j+1}, i.e. $j + 1/2$. The intensity at this point, I^0_i, is related to the intensities $I_{i,j}$ and $I_{i,j+1}$ at the boundaries, j and $j+1$, by

$$I^0_i = (I_{i,j} + I_{i,j+1})/2. \tag{27}$$

The intensity I^0_i is related to the intensities $I^0_{i-1/2}$ and $I^0_{i+1/2}$ at the angular edges $i - 1/2$ and $i + 1/2$ by

$$I^0_i = (I^0_{i-1/2} + I^0_{i+1/2})/2. \tag{28}$$

The evaluation of Eq. (26) is performed from $r = r_s$ to $r = r_w$ (i.e. inwards) for $\mu_i < 0$ and from $r = r_w$ to $r = r_s$ (i.e. outwards) for $\mu_i > 0$ as described in the following.

$\mu_i < 0$ (*inward calculation*)

Eliminating $I_{i,j}$ and $I^0_{i+1/2}$ from Eq. (26) by utilizing the relations given by Eqs. (27) and (28), we obtain

$$I^0_i = \frac{\mu_i A I_{i,j+1} + CI^0_{i-1/2} - B(k_aI^0_b - k_sI^0_s)}{\mu_i A + C - B(k_a - k_s)}, \quad \mu_i < 0, \tag{29}$$

where $A = A_j + A_{j+1}$, $C = (A_{j+1} + A_j)\frac{\alpha_{i+1/2}+\alpha_{i-1/2}}{w_i}$.

$\mu_i > 0$ (*outward calculation*)

Eliminating $I_{i,j+1}$ and $I^0_{i+1/2}$ from Eq. (26) by utilizing the relations given by Eqs. (27) and (28), we obtain

$$I^0_i = \frac{\mu_i A I_{i,j} - CI^0_{i-1/2} + B(k_aI^0_b - k_sI^0_s)}{\mu_i A - C + B(k_a - k_s)}, \quad \mu_i > 0, \tag{30}$$

Considering the two boundary surfaces to be diffusely emitting–reflecting, the boundary condition for the above Eq. (19) can be expressed in discrete ordinates form as

$$\text{at } r = r_w : I_i = \varepsilon_w I_{b,w} + \frac{1-\varepsilon_w}{\pi}\sum_{i'} w_{i'}|\mu_{i'}|I_{i'}, \quad (\mu_i > 0,\ \ \mu_{i'} < 0), \tag{31}$$

$$\text{at } r = r_s : I_i = \varepsilon_s I_{b,s} + \frac{1-\varepsilon_s}{\pi}\sum_{i'} w_{i'}|\mu_{i'}|I_{i'}, \quad (\mu_i < 0,\ \ \mu_{i'} > 0). \tag{32}$$

The evaluation of Eqs. (29) and (30) requires an initial value of the intensity $I^0_{1/2}$. This value may be found by solving Eq. (22) in the direction, where the angular derivative vanishes, i.e. $\eta = 0$. With an assumed intensity distribution at an arbitrary point r_j (or r_{j+1}), the intensities I^0_i at the center of the range (r_j, r_{j+1}) can be evaluated, with which the intensity distribution at the next point r_{j+1} (or r_j) can be calculated.

Finally, the divergence of the radiative heat flux which is necessary for solving the energy equation (8) may be approximated by

$$\nabla\cdot\dot{q}_r \approx k_a\left(4\sigma T^4 - \sum_i w_i I_i\right). \tag{33}$$

For the one-dimensional cylindrical medium with symmetry conditions, we have

$$I(r,\theta,\psi) = I(r,-\theta,\psi) = I(r,\theta,-\psi). \tag{34}$$

Therefore, the intensity is the same for positive and negative values of ξ, as well as for positive and negative values of η. Thus, we only need to consider positive values of ξ_i and η_i, leading to $M = N(N+2)/4$ different ordinates, with quadrature weights $w_i'' = 4w_i$.

3.4. Numerical solution

Eq. (8) for the transient temperature field around the heated wire and Eqs. (29) and (30) for the steady-state radiation transfer are solved numerically by the implicit finite difference method (IFD). In order to reduce the calculation time maintaining a sufficiently high accuracy, the one-dimensional cylindrical geometry is divided into concentric cylinders $(r_0, r_1, \ldots, r_J)$ with a progressive size of the elements $(r_{j+1} = r_j \cdot U,\ U > 1)$. In this way, we get a fine grid of points close to the wire, where large gradients of temperature and intensity exist.

With an assumed radiative source term, $\nabla \cdot \dot{q}_r$, and knowing the actual temperature distribution within the medium, the temperature distribution at the respective next time step is calculated by Eq. (8), and from the obtained temperature field the radiation field can be updated by Eqs. (29) and (30). This iteration runs until the temperature difference between two consecutive iterative steps is less than some limiting value specified by an accuracy parameter.

Several S_N quadratures have been tested. Finally, we decided to use the S_4 that provides sufficiently high accuracy and requires the smallest calculation time.

3.5. Validity tests with the numerical solution

The numerical solution of the conduction–radiation problem has been tested for the limiting cases of an extremely high and a zero extinction coefficient. These accuracy tests were carried out with the following parameters: $\lambda_c = 0.0346$ W/m K, $\rho c_p = 135.2 \times 10^3$ J/m^3 K, $r_w = 0.25 \times 10^{-3}$ m, $r_s = 0.05$ m, $\varepsilon_w = 0.1; 1.0$, $\dot{Q}_l = 1.0$ W/m.

For assessing the accuracy of the numerical-solution method, it is desirable to use an analytical solution to the problem as a reference. The only analytical solution which is available is that for vanishing radiative transfer which means the extinction coefficient E goes to infinite (opaque limit) as given by [12]

$$\Delta T(r,t) = \frac{\dot{Q}_l}{2\pi\lambda_c}\ln\left(\frac{r_s}{r}\right) + \frac{\dot{Q}_l}{2\lambda_c r_w}\sum_{i=1}^{\infty}\exp(-\kappa\beta_i^2 t) \times \frac{J_0^2(r_s\beta_i)[J_0(r\beta_i)Y_1(r_w\beta_i) - Y_0(r\beta_i)J_1(r_w\beta_i)]}{\beta_i[J_1^2(r_w\beta_i) - J_0^2(r_s\beta_i)]}, \tag{35}$$

where β_i are roots of $J_1(r_w\beta_i)Y_0(r_s\beta_i) - Y_1(r_w\beta_i) \times J_0(r_s\beta_i) = 0$.

In order to compare the numerical solution with that of Eq. (35), we carry out two calculations. The first one delivers an exact numerical solution and it can be obtained by application of boundary conditions, Eqs. (10)–(12), to Eq. (8) and setting $\dot{q}_r = 0$. The result has been compared with Eq. (35) and the difference is found to be less than 0.15% in the entire range of times 1–600 s, and less than 0.05% in the experimentally interesting range 100–600 s (see Fig. 1). By this the high accuracy of the applied IFD-method, the kind of grid and time step is clearly confirmed (Fig. 1).

As the second test, Eqs. (8), (29) and (30) have been solved with a very large value of the extinction coefficient, $E = 1,000,000/\text{m}$, which delivers the discrete ordinates solution of the combined conductive and radiative heat transfer. The difference between this S_4-approximation and the analytical solution is also found to keep below 0.15% and 0.05% respectively (Fig. 1).

A further test of the numerical solution of the combined conduction and radiation heat transfer can be made at the other limit of the extinction coefficient, i.e. the transparency limit ($E = 0$). In the case of transparency, the radiative contribution to the heat flux may be evaluated independently of the conductive heat transfer, because the medium does not participate and there is a direct radiative exchange between the surfaces of the wire and of the outer boundary of the sample. The radiative heat flux at $r = r_w$ depends only on the temperatures and the emissivities of both surfaces, and is expressed as [7]

$$\dot{q}_r(r_w) = \frac{\sigma(T_w^4 - T_s^4)}{\dfrac{1}{\varepsilon_w} + \dfrac{r_w}{r_s}\left(\dfrac{1}{\varepsilon_s} - 1\right)}. \tag{36}$$

The numerical solution, in this case, is obtained from Eq. (8) by setting $\nabla \cdot \dot{q}_r = 0$ and substituting the radia-

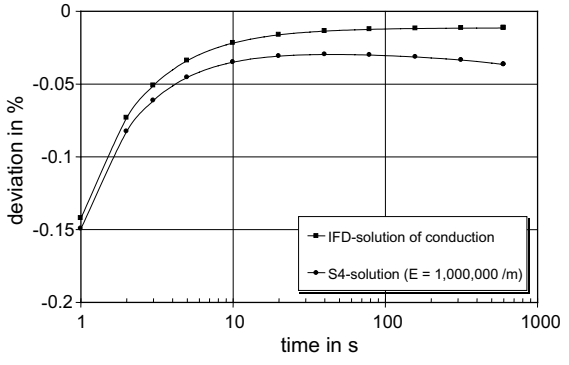

Fig. 1. Deviation of IFD-solution (without radiation term for conduction case) and S_4-solution (with radiation term and a very high extinction coefficient like a conduction case) from the exact solution [12].

tive heat flux determined by Eq. (36) into the boundary condition Eq. (11). The result is compared with the numerical solution of the combined conduction–radiation problem by solving Eqs. (8), (29) and (30), where the extinction coefficient is set to zero ($E = 0$). The agreement is found to be very good with overall deviations less then 0.001% in the time range 1–600 s.

At this point, we can conclude that the numerical solution of the combined conductive and radiative heat transfer using the discrete ordinates solution method for the radiative transport is highly accurate in the limiting cases of the extinction coefficient ($E = 0$ and $E \to \infty$). By an additional test with the differential-approximation method for solving the radiative transfer equation (see [14]) which, however, can only be applied in cases of a high extinction coefficient, good agreement is found with the S_4-approximation for $E > 5000$/m ($\vartheta_0 = 25$ °C) and $E > 10,000$/m ($\vartheta_0 = 500$ °C).

4. Results and discussions

4.1. Time-dependent temperature rise of the hot wire

As an example for the numerical simulation of hot-wire experiments, the time-dependent temperature rise of the wire has been evaluated for various extinction coefficients starting from thermal equilibrium at $\vartheta_0 = 25$ °C (further parameters as applied in the validity tests). Fig. 2 shows the excess temperature vs. the logarithm of time for a wire with the emissivity $\varepsilon_w = 0.1$.

With the extinction coefficient $E \to \infty$ we have the limiting case of radiation exchange between the wire and the medium next to it with a penetration length $l_m = 0$ m, i.e. both of the partners exhibit the same temperature and there is no contribution due to radiation. This corresponds to an exclusively conducting medium, and the typical straight-line behaviour is obtained in Fig. 2 as well known from hot-wire experiments. When the extinction coefficient is being decreased starting from $E = \infty$, the penetration length begins to arise from zero and the process of radiation exchange starts to contribute to the total heat transfer. The time-dependent temperature rise of the wire is reduced due to this additional cooling. This effect is clearly visible in Fig. 2, where the slopes of the curves decrease when the extinction coefficient is stepwise reduced from $E = \infty$ to $E = 5000 \ldots 1000 \ldots 500 \ldots 100$/m corresponding to an increase of the penetration length from $l_m = 0$ to $l_m = 0.2 \ldots 1 \ldots 2 \ldots 10$ mm. In course of this, the wire comes into a radiation exchange with increasingly adjacent parts of the sample, and the same holds for any location inside the sample itself. Special conditions arise for the radiation process close to the outer boundary which is assumed to be a black emitter–absorber coming also into a direct radiation exchange with increasing parts of the sample. Simultaneously, the radiation emitted by the sample per volume decreases with the extinction coefficient (Eq. (15)) whereas the radiation flux emitted by the outer boundary keeps constant. This brings an increasing resistance to the total radiation. As a result, the slope of the curves is modified with the tendency to increase again when the extinction coefficient is reduced below $E = 500 \ldots 100$/m. In case of $E = 10$/m, e.g., the penetration length amounts to $l_m = 100$ mm and a direct radiation exchange between the wire and the outer boundary is obtained. Finally, if E is reduced to zero, the sample itself does not any longer participate, and the remaining difference between the curves for $E = 0$ and ∞ is simply due to the direct radiation exchange from the wire to the outer boundary.

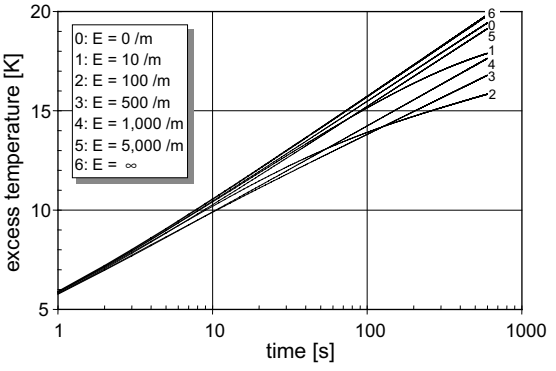

Fig. 2. Time-dependent excess temperature of the hot wire (for $\vartheta_0 = 25$ °C, $\dot{Q}_l = 1$ W/m, and $\varepsilon_w = 0.1$).

4.2. Radial temperature profile

Fig. 3 shows radial profiles of the excess temperature for $E = 100$/m and 10,000/m respectively. Results have been evaluated for two types of the wire, one with low emissivity $\varepsilon_w = 0.1$ and one corresponding to a black body. In the core of the sample surrounding the heated wire, a logarithmic temperature profile is obtained which is well known for the case of unsteady-state conduction. This core region expands from one time step to the next along with the rising local temperatures, which are found to be higher for the larger extinction coefficient due the reduction of radiation exchange. The effect of the wire emissivity upon the temperature profile is small especially for large extinction coefficients where the radiation exchange is small. For $E = 100$/m, however, at short times an enhanced cooling effect can be seen for $\varepsilon_w = 1.0$, which seems to disappear after, maybe, 600 s.

4.3. Radial distribution of the radiative flux

The radial distribution of the radiative flux within the sample is plotted in Figs. 4 and 5 depending on various

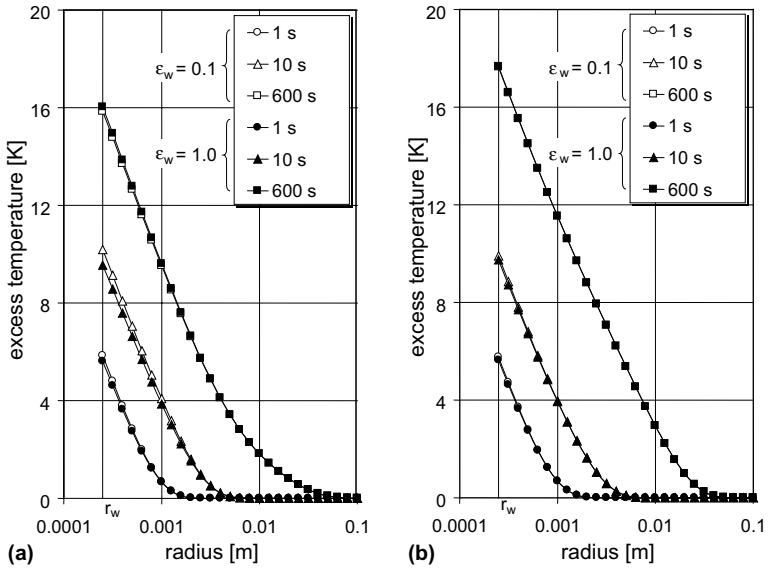

Fig. 3. Radial profiles of the excess temperature in the sample (for $\vartheta_0 = 25$ °C and $\dot{Q}_l = 1$ W/m) with the extinction coefficient (a) $E = 100$/m, (b) $E = 10,000$/m.

parameters. Fig. 4a shows results for $\vartheta_0 = 25$ °C and $E = 100$/m at three different times. For such a small extinction coefficient and at such a short time after starting the numerical experiment, the radiative emission from the medium is generally low. If the wire has a high emissivity ($\varepsilon_w = 1$, see the full circles and triangles), the profile of radiative flux is similar to the transparency (i.e. nonparticipating) case, where it decreases inversely with the radius. For low emissivity of the wire ($\varepsilon_w = 0.1$, see the empty circles and triangles), the overall radiative heat flux is extremely small, because both the wire and the medium radiate very weak.

For larger times, e.g., for 600 s, the radiative-flux profile is influenced by the time-dependent temperature variations where not only the wire itself but also wide ranges of the adjacent sample show enhanced temperatures and emission of radiation, too. Due to the large penetration length, radiation originating from a big volume is being emitted evenly in all directions—also backward to the wire which, being a black body in case of $\varepsilon_w = 1$, has to absorb all the irradiated energy. The balance is found to be negative (see Fig. 4a) at long times especially for $\varepsilon_w = 1$ and in a reduced extend for $\varepsilon_w = 0.1$ too. Due to this, a maximum of the radiative flux is obtained at a distance from the wire surface which is something smaller than the penetration length. Outside this range, i.e. at a larger radius, this effect disappears. Of course, the first and second laws of thermodynamics require a respective enhancement of the conduction heat transfer from the wire in cases of a negative radiation flux, which indeed has been received

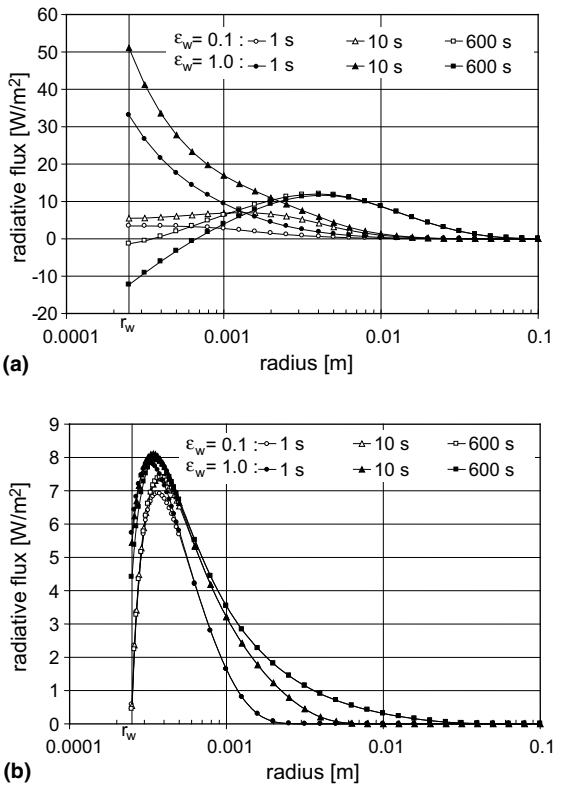

Fig. 4. Radial distribution of the radiative flux in the sample (for $\vartheta_0 = 25$ °C, $\dot{Q}_l = 1$ W/m) with the extinction coefficient (a) $E = 100$/m, (b) $E = 10,000$/m.

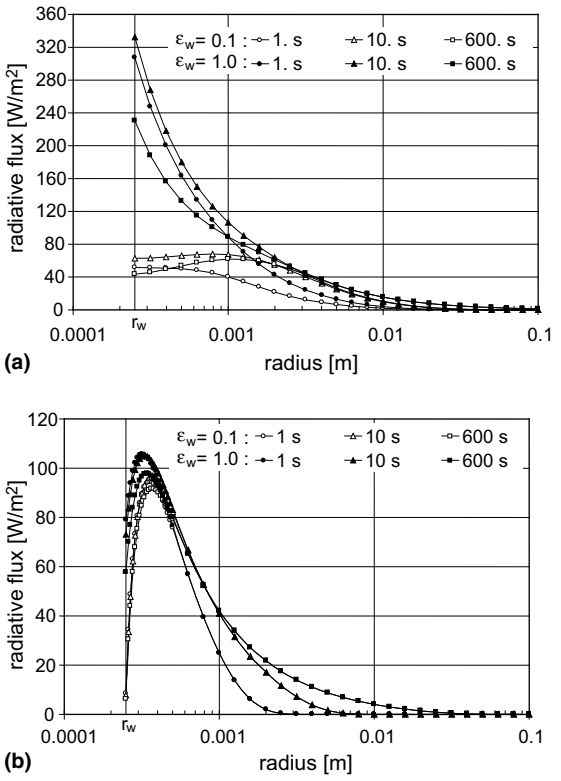

Fig. 5. Radial distribution of the radiative flux in the sample (for $\vartheta_0 = 500$ °C, $\dot{Q}_l = 1$ W/m) with the extinction coefficient (a) $E = 100/\mathrm{m}$, (b) $E = 10,000/\mathrm{m}$.

in such situations (for this, see [14]). These phenomena clearly show the non-diffusive character of the radiation, especially close to the wire.

For a higher value of the extinction coefficient, $E = 10,000/\mathrm{m}$, the negative radiative flux vanishes, as shown in Fig. 4b, because the mean penetration distance is very small in this case. Only the radiation of a very small region close the wire can reach the wire in the negative direction, and the total radiation energy from the sample to the wire is also very small. It is slightly influenced by the emissivity of the wire and a maximum radiation flux is obtained at a distance of about 0.1 mm from the wire surface which exactly corresponds to the penetration length. In this case the radiation heat transfer becomes much more diffusively than for $E = 100/\mathrm{m}$.

In the high temperature range the radiation flux is strongly increased according to the Stefan–Boltzmann law. Fig. 5a shows numerical results for $\vartheta_0 = 500$ °C and $E = 100/\mathrm{m}$. In this case the wire and also the adjacent parts of the sample have high temperatures. Both of them are very active emitters and the resulting radiative flux is much higher than at $\vartheta_0 = 25$ °C (see Fig. 4a) with only positive values, i.e. it is exclusively directed away from the wire. Again there is a radiative-flux decrease with time near the wire and also a strong wire-emissivity effect. The radiative flux distribution for the extinction coefficient $E = 10,000/\mathrm{m}$, shown in Fig. 5b, looks like the one at low temperature $\vartheta_0 = 25$ °C, but the influence of the wire emissivity is stronger. The radiative heat transfer stays still far from being a diffusive process.

4.4. Time-dependent radiative flux

Due to the principle, the temperature of the heated wire is caused to increase during the experiment and with it, the radiative heat flux at the wire must increase if the radiative heat transfer is a diffusive one. Fig. 6a shows radiative-flux transients at the wire for $\vartheta_0 = 25$ °C and $\varepsilon_w = 0.1$. For small extinction coefficients ($E = 100/\mathrm{m}$, $1000/\mathrm{m}$) the radiative heat flux initially shows an increase, but after passing through a maximum at 12 and 3 s respectively it decreases due to the transient radiation effects described above. The minimum extinction coefficient which is required for a monotonic increase of the radiative heat flux amounts to $E = 10,000/\mathrm{m}$ for $\vartheta_0 = 25$ °C and even $E = 100,000/\mathrm{m}$ for $\vartheta_0 = 500$ °C (see Fig. 6b).

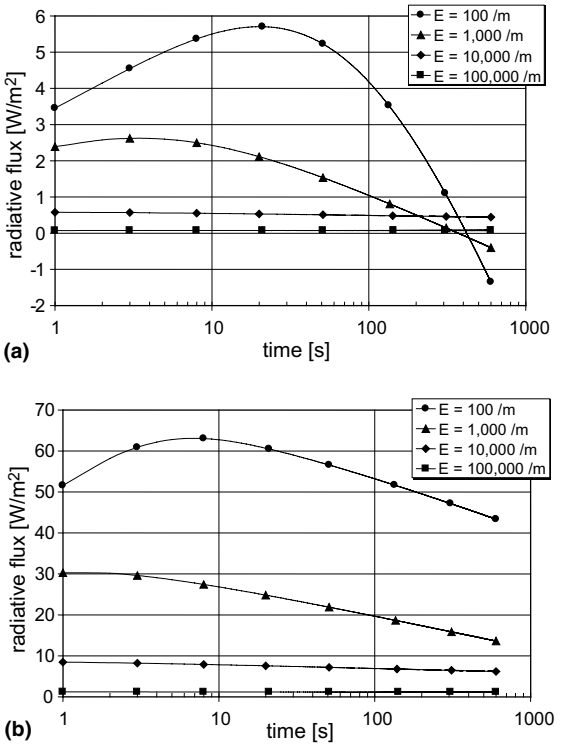

Fig. 6. Time-dependent radiative flux at the wire ($\dot{Q}_l = 1$ W/m, $\varepsilon_w = 0.1$) for (a) $\vartheta_0 = 25$ °C, (b) $\vartheta_0 = 500$ °C.

4.5. Derivation of the effective thermal conductivity

For assessing the accuracy of a numerical hot-wire experiment the effective thermal conductivity gained from the evaluated time-dependent temperature rise of the wire (using Eq. (7)) has to be compared with the effective thermal conductivity calculated as the sum of the pure thermal conductivity and the radiative conductivity derived from the Rosseland diffusion model:

$$\lambda_{\mathrm{app,measure}} = \frac{Q}{4\pi}\cdot\frac{\ln t_2 - \ln t_1}{T_2 - T_1} \stackrel{?}{=} \lambda_{\mathrm{app,diff}} = \lambda_{\mathrm{c}} + \frac{16\sigma}{3E}T_{\mathrm{r}}^3.$$

The temperatures, T_1 and T_2, are taken for the time interval between $t_1 = 120$ s and $t_2 = 600$ s which is typical for actual practice. For the radiation temperature, T_{r}, the initial temperature, $T_0 = \vartheta_0 + 273.15$ K, is used here, and the reference temperature of the measured thermal conductivity must also be T_0.

The deviation between both values of the effective thermal conductivity

$$\frac{\lambda_{\mathrm{app,measure}} - \lambda_{\mathrm{app,diff}}}{\lambda_{\mathrm{app,diff}}}\cdot 100\%$$

is plotted vs. the heating power per unit length in Fig. 7 for three different temperatures with the extinction coefficient and wire emissivity as the parameters. The deviation is found to increase linearly with the heating power starting from the negative (i.e. an underdetermination of the effective thermal conductivity) for all of the three temperatures investigated, and a strong influence of the emissivity is found if the extinction coefficient keeps below $E = 5000$/m (for $\vartheta_0 = 25$ °C, see Fig. 7a). For the higher temperatures (Fig. 7b and c) respective limits are found to be around $E = 50,000$/m. In addition, the large influence of the emissivity of the wire observed in these cases means a dependence of the measured results on the measurement arrangement bringing measured results which are not really properties of the sample.

The negative deviations vanish for very large values of E. That means, we should use the hot-wire method only for measuring samples with a large enough E. The linear relationship between the measured effective thermal conductivity and the heating power per unit length observed in experiments [13] are confirmed by calculated results of this work, as shown in Fig. 7. The true value of the effective thermal conductivity can be obtained by extrapolation of the line of linear relationship to zero heating power per unit length. Measurements of sample with low E will, however, deliver the true thermal conductivity only when a large enough heating power is supplied. This may lead to the opinion that hot-wire measurements are also possible for low values of E. The measured results, however, are dependent on the measurement arrangement and they are not physical properties of the sample.

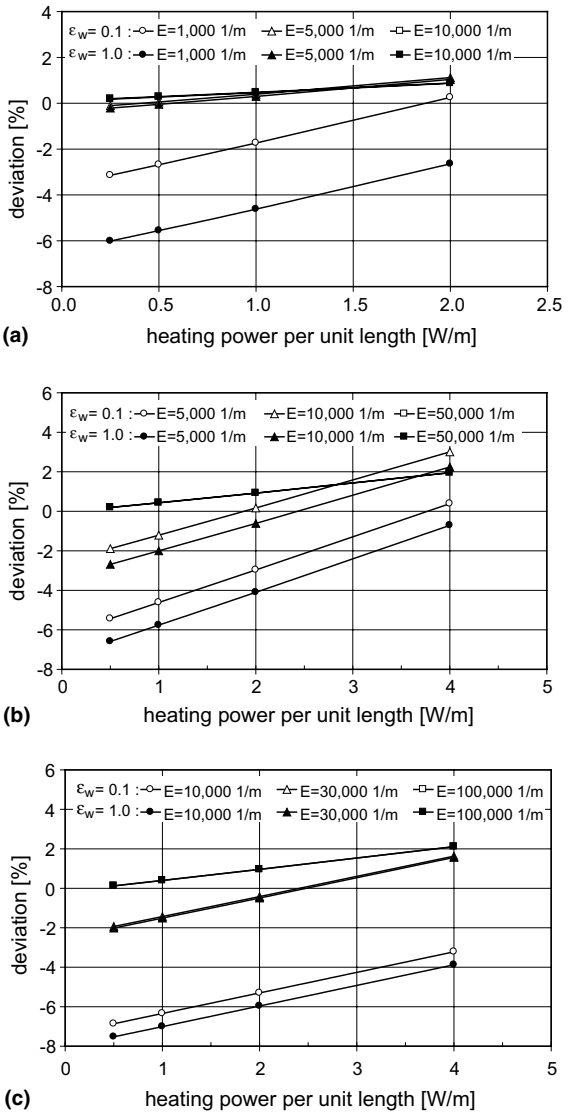

Fig. 7. Deviation between the thermal conductivities as "measured" from the simulated time history and calculated from the diffusion model for (a) $\vartheta_0 = 25$ °C, (b) $\vartheta_0 = 500$ °C, (c) $\vartheta_0 = 1000$ °C (with the initial temperature for reference).

In actual practice, one usually uses the mean temperature as reference for the measured thermal conductivity. Fig. 8 shows that for samples with a sufficiently large extinction coefficient, depending on the temperature, the mean temperature averaged from the temperatures of the wires at two measurement points, T_1, and T_2, can be used as reference temperature without obtaining any heating power effect.

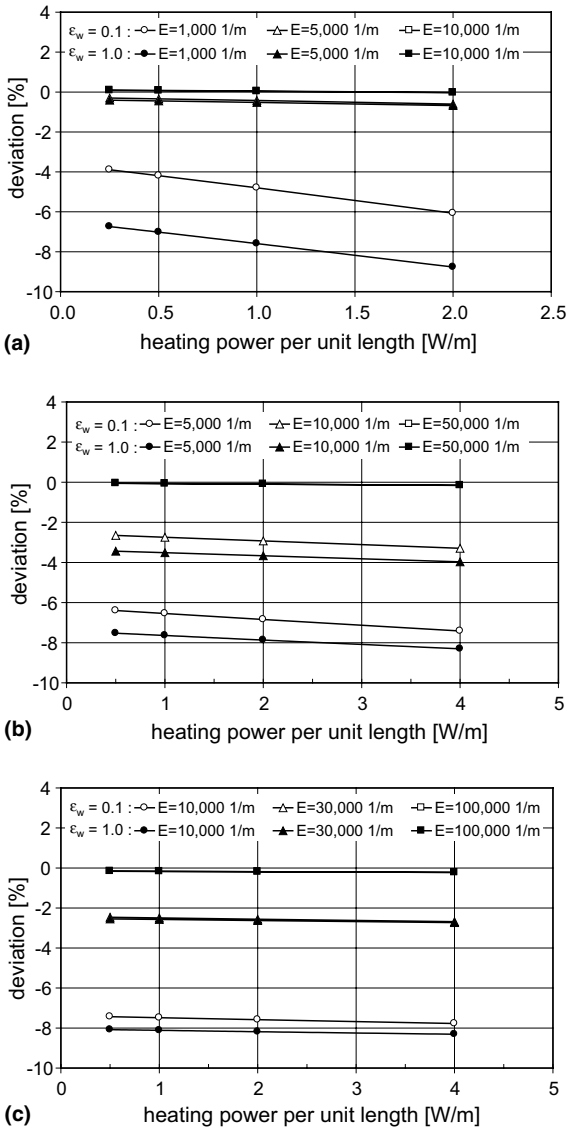

Fig. 8. Deviation between the thermal conductivities as "measured" from the simulated time history and calculated from the diffusion model for (a) $\vartheta_0 = 25$ °C, (b) $\vartheta_0 = 500$ °C, (c) $\vartheta_0 = 1000$ °C (with the mean temperature for reference).

5. Conclusions

The finite difference method is a convenient method for solving the equations of heat transfer in absorbing and emitting media. With the discrete-ordinates method the radiation-transfer equation can be easily solved so that the numerical simulation is suitable for extensive parameter studies and the influence of radiation on measurements of thermal conductivity in case of the hot-wire method can be studied efficiently. The extinction coefficient of the sample is a very important parameter for the accuracy of measurement, and it brings an underdetermination of the thermal conductivity if it is too small. The range of extinction coefficients, in which thermal conductivity can be measured accurately, shifts to larger values when the measurement temperature increases. Here are some examples of the recommended range of the extinction coefficient derived from the calculated results:

for $\vartheta_0 = 25$ °C: $E \geqslant 10,000$/m
for $\vartheta_0 = 500$ °C: $E \geqslant 50,000$/m
for $\vartheta_0 = 1000$ °C: $E \geqslant 100,000$/m

Results of the numerical simulation confirmed the linear relationship between the measured effective thermal conductivity and the heating power observed in experiments. Extrapolation to the heating power zero allows for the determination of the thermal conductivity if the initial temperature is chosen as the reference. This method needs, however, several hot-wire measurements and is, therefore, not efficient. Instead of this, one can easily use the mean temperature as the reference for the measured thermal conductivity.

Acknowledgements

The support of this work by the Deutsche Forschungsgemeinschaft (DFG) is greatly appreciated.

References

[1] J.J. Healy, J.J. de Groot, J. Kestin, The theory of the transient hot-wire method for measuring thermal conductivity, Physica 82C (1976) 392–408.
[2] A. Saito and J.E.S. Venart, Radiation effects with the transient line source measurement of fluid thermal conductivity, in: Proceedings of the 6th International Heat Transfer Conference, Washington, DC, USA, 1978, pp. 79–84.
[3] A. Saito, Review of the transient line source technique, Bull. JSME 23 (183) (1980) 1459–1466.
[4] J. Menashe, W.A. Wakeham, Effect of absorption of radiation on thermal conductivity measurements by the transient hot-wire technique, Int. J. Heat Mass Transfer 25 (5) (1982) 661–673.
[5] C.A. Nieto de Castro, S.F.Y. Li, G.C. Maitland, W.A. Wakeham, Thermal conductivity of toluence in the temperature range 35–90 °C at pressures up to 600 MPa, Int. J. Thermophysics 4 (4) (1983) 311–327.
[6] H.P. Ebert, J. Fricke, Influence of radiation transport on hot-wire thermal conductivity measurements, High Temp.–High Pressures 30 (1998) 655–669.
[7] R. Siegel, J.R. Howell, Thermal Radiation Heat Transfer, third ed., Taylor & Francis, 1992.
[8] R. Viskanta, R.J. Grosh, Heat transfer by simultaneous conduction and radiation in an absorbing medium, ASME J. Heat Transfer 84 (1) (1962) 63–72.

[9] F. Yu, X. Zhang, X. Yin, Z. Gao, Simultaneous conduction and radiation in semitransparent media for transient hot-wire experiments, High Temp.–High Pressures 30 (1998) 105–111.
[10] B.G. Carlson, K.D. Lathrop, Transport theory—The method of discrete ordinates, in: H. Greenspan, C.N. Kelber, D. Okrent (Eds.), Computing Methods in Reactors Physics, Gordon and Breach Science Publishers, New York, 1968.
[11] M.F. Modest, Radiative Heat Transfer, McGraw-Hill, Inc., 1993.
[12] H.S. Carslaw, J.C. Jaeger, Conduction of Heat in Solids, Clarendon Press, Oxford, 1948.
[13] E.I. Aksel'rod, I.I. Vishnevskii, Use of the hot wire method for measuring the thermal conductivity of light-weight, fiber and powder refractory materials. Ukrainian Scientific-Research Institute of Refractories. Translated from Ogneupory, No. 4, 1984, pp. 49–53.
[14] L.T.S. Tran, Strahlungseffekte bei instationären Heizdrahtmessungen an porösen Wärmedämmstoffen. Doctoral Dissertation, Technische Universität Bergakademie Freiberg, Germany, 2002.